New derivatives from dehydrodieugenol B and its methyl ether displayed high anti-Trypanosoma cruzi activity and cause depolarization of the plasma membrane and collapse the mitochondrial membrane potential

Thalita S Galhardo, Anderson K Ueno, Thaís A Costa-Silva, André G Tempone, Wagner A Carvalho, Cedric Fischmeister, Christian Bruneau, Dalmo Mandelli, João Henrique G Lago

New derivatives from dehydrodieugenol B and its methyl ether displayed high anti-*Trypanosoma cruzi* activity and cause depolarization of the plasma membrane and collapse the mitochondrial membrane potential

Thalita S. Galhardo[a,*] Anderson K. Ueno[b,*], Thaís A. Costa-Silva[a,c], André G. Tempone[d], Wagner A. Carvalho[a], Cedric Fischmeister[e], Christian Bruneau[e], Dalmo Mandelli[a,**], João Henrique G. Lago[a,**]

[a]*Center of Natural and Human Sciences, Federal University of ABC, Santo Andre, 09210-580, Brazil.*

[b]*Institute of Environmental, Chemical and Pharmaceutical Sciences, Federal University of São Paulo, Diadema, 09972-270, Brazil.*

[c]*SENAI Institute of Inovation in Biotecnology, 01130-000, São Paulo, Brazil.*

[d]*Centre for Parasitology and Mycology, Instituto Adolfo Lutz, São Paulo, 01246-000, Brazil.*

[e]*Institut des Sciences Chimiques de Rennes, University of Rennes, Rennes, UMR6226, 35000, France.*

*These authors contributed equally.

** Corresponding authors. *Tel: (+5511) 49960001. Fax: (+5511) 49963166.

E-mail address: joao.lago@ufabc.edu.br and dalmo.mandelli@ufabc.edu.br

ABSTRACT

In the present work, dehydrodieugenol B (**1**) and its methyl ether (**2**), isolated from *Nectandra leucantha* twigs, were used as starting material for the preparation of two new derivatives (**1a** and **2a**) containing an additional methoxycarbonyl unit on allyl side chains. Compounds **1a** and **2a** demonstrated activity against trypomastigotes (EC_{50} values of 13.5 and 23.0 M, respectively) and against intracellular amastigotes (EC_{50} values of 10.2 and 6.1 M, respectively). Additionally, compound **2a** demonstrated no mammalian cytotoxicity up to 200 M whereas compound **1a** exhibited a CC_{50} value of 139.8 M. The mechanism of action studies of compounds **1a** and **2a** demonstrated a significant depolarization of the plasma membrane potential in trypomastigotes, followed by a mitochondrial membrane potential collapse. Neither calcium level nor reactive oxygen species alterations were observed after a short-time incubation. Considering the potential of compound **2a** against *T. cruzi* and its simple preparation from the natural product **2**, isolated from *N. leucantha*, this compound could be considered a new hit for future drug design studies in Chagas disease.

Keywords: *Trypanosoma cruzi*, neolignans, plasma membrane; mitochondrial membrane.

1. Introduction

Currently, about one billion people in the world suffer from at least one of the 20 diseases that are classified by WHO as Neglected Tropical Diseases (NTDs) [1]. These diseases represent a major cause of morbidity and mortality, mainly in tropical regions of the world and, are considered neglected due to a lack of financial investments in the Research & Development for development of new drugs [2]. A recent study showed that among the tropical parasitic diseases that cause mortality in the Brazilian population, Chagas disease deserves important attention [3]. Caused by the flagellate protozoan parasite *Trypanosoma cruzi*, there are only two available drugs for the treatment: benznidazole and nifurtimox [4]. To contribute to novel therapies, the chemistry of natural products plays an important role in the search for bioactive compounds [5-7]. The genus *Nectandra* is composed of approximately 120 species of predominantly tropical distribution, with wide diversity in the Brazilian Atlantic Forest [8,9]. Phytochemical studies performed with *Nectandra* species have shown great structural diversity of bioactive metabolites, including lignoids, alkaloids, and terpenoids [8]. *N. leucantha*, a species with occurrence in the Atlantic Forest of the São Paulo and the Espírito Santo States of Brazil, accumulated different neolignans formed by oxidative coupling of eugenol with anti-inflammatory, antitumoral, and antiparasitic potential, especially against *Leishmania infantum* and *Trypanosoma cruzi* [7, 9-14]. In the present work, two new methoxycarbonyl derivatives of dehydrodieugenol B and methyldehydrodieugenol B, both isolated from twigs of *N. leucantha*, were prepared via olefin cross-metathesis with methyl acrylate in the presence of a ruthenium-based catalyst. Obtained compounds were evaluated against extra (trypomastigote) and intracellular (amastigote) forms of *T. cruzi*. Moreover, the

phenotypical mechanisms involved in the parasite death of these compounds in trypomastigotes of *T. cruzi* were also investigated.

2. Material and methods

2.1 General experimental procedures

Methylacrylate was purchased from Sigma-Aldrich and stored over 3 Å molecular sieves under an inert atmosphere. Dimethyl carbonate was purchased from Alfa-Aesar and was distilled under an inert atmosphere of argon and stored over 3Å molecular sieves. Hoveyda-Grubbs II catalyst M72 (C627) was provided by Umicore. Column chromatography (CC) was performed with silica gel (230−400 mesh, Merck) and Sephadex LH-20 (Aldrich), while thin layer chromatography (TLC) separations were carried out on silica gel 60 PF_{254} (Merck). ^{1}H and ^{13}C nuclear magnetic resonance (NMR) spectra were recorded, respectively, at 400 and 100 MHz on a Bruker Avance III Ascend 400 spectrometer using $CDCl_3$ (Sigma-Aldrich) as the solvent and using the residual signal of $CHCl_3$ as the internal standard (δ 7.26 vs TMS). Electrospray ionization - high resolution mass spectrometry (ESI-HRMS) data were measured on an Agilent 6510 Q-TOF LC/MS spectrometer, using an ESI ion source operating at positive mode. Elemental analysis was obtained in a Perkin-Elmer Elemental Analyzer model 2400 CHN. Infrared (IR) spectra were recorded with a Shimadzu FT-IR Prestige-21 instrument.

2.2. Plant material

Fresh twigs of *N. leucantha* were collected at Cubatão city, São Paulo State, in March 2019 from the same previously studied species [12,13]. The plant species was identified by Dr. Euder G.A. Martins and a voucher specimen (EM357) has been deposited in the Herbarium of the Institute of Biosciences, University of São Paulo, SP, Brazil.

2.3. Extraction and isolation

Dried and powdered twigs of *N. leucantha* (200 g) were extracted with *n*-hexane (10 x 250 mL). Combined organic extracts were concentrated under reduced pressure to afford 7.5 g of crude extract. Part of this extract (1.5 g) was chromatographed over a silica gel column eluted with increasing amounts of EtOAc in *n*-hexane to afford five fractions (A - E). Fraction C (396 mg) was composed of pure **2**. Part of the fraction D (375 mg) was chromatographed over Sephadex LH-20, eluted with $CHCl_3$:MeOH 1:1, to afford pure compound **1** (287 mg).

*2.4. Preparation of compounds **1a** and **2a** via olefin cross-metathesis reaction.*

A dry and degassed Schlenk tube was loaded under argon with 50 mg of compound **1** or **2** (0.15 mmol, 1 equiv.), 1.6 mg of *p*-benzoquinone (1.5×10^{-2} mmol), 56 µL of methyl acrylate (0.61 mmol, 4 equiv.), and 1.5 mL of dimethyl carbonate (DMC). Another dry and degassed Schlenk tube was loaded under argon with 1.9 mg of Hoveyda-Grubbs II catalyst (3×10^{-3} mmol, 2 mol%) and 0.5 mL of DMC. The ruthenium catalyst was then

taken by a syringe and was slowly added into the first Schlenk tube through the septum by means of a syringe pump for 2 h at 80°C. After addition, the reaction mixture was stirred at 80 °C for an additional time (3 h) [15]. After solvent evaporation under reduced pressure, products **1a** or **2a** were individually purified by chromatography column over silica gel eluted with increasing amounts of EtOAc in *n*-hexane.

*2.4.1. Methyl 4-{4-[2-hydroxy-3-methoxy-5-(4-methoxy-4-oxobut-2E-en-1-yl)phenoxy]-3-methoxyphenyl}but-2E-enoate (**1a**):* yellowish oil (yield 42%). IR (KBr) ν_{max} 3421, 2947, 2837, 1720, 1654, 1585, 1508, 1429, 1269, 1211, 1155, 1093, 1033, 827 cm^{-1}; ^{1}H NMR ($CDCl_3$, 400 MHz): δ/ppm 7.09 (1H, dt, *J* = 15.7 and 6.7 Hz, H-8), 7.02 (1H, dt, *J* = 15.5 and 6.8 Hz, H-8') 6.88 (1H, d, *J* = 8.1 Hz, H-6'), 6.76 (1H, d, *J* = 8.1 Hz, H-3'), 6.69 (1H, d, *J* = 8.1 Hz, H-2'), 6.46 (1H, d, *J* = 1.7 Hz, H-2), 6.35 (1H, d, *J* = 1.7 Hz, H-6), 5.84 (1H, br d, *J* = 15.7 Hz, H-9), 5.81 (br s, OH) 5.77 (1H, br d, *J* = 15.5 Hz, H- 9'), 3.89 (3H, s, H-10), 3.85 (3H, s, H-10'), 3.73 (3H, s, H-12), 3.71 (3H, s, H-12'), 3.49 (2H, d, *J* = 6.8 Hz, H-7'), 3.37 (2H, d, *J* = 6.7 Hz, H-7); ^{13}C NMR ($CDCl_3$, 100 MHz): δ/ppm 167.0 (C-11/11'), 150.7 (C-5'), 148.2 (C-5), 147.8 (C-8'), 147.5 (C-8), 144.6 (C-3), 144.5 (C-4'), 135.7 (C-4), 134.2 (C-1'), 128.8 (C-1), 122.1 (C-9'), 121.9 (C-9), 121.3 (C-2'), 119.8 (C-3'), 113.2 (C-6'), 112.1 (C-6), 107.5 (C-2), 56.4 (C-10), 56.2 (C-10'), 51.7 (C-12), 51.6 (C-12'), 38.3 (C-7/7'); ESI-HRMS *m/z* 465.1519 $[M + H]^+$ (calcd. for $C_{24}H_{26}O_8Na$ 465.1525); Anal. C 64.92, H 6.01% (calcd. for $C_{24}H_{26}O_8$, C 65.15, H 5.92%).

*2.4.2. Methyl 4-{4-[2,3-dimethoxy-5-(4-methoxy-4-oxobut-2E-en-1-yl)phenoxy]-3-methoxyphenyl}but-2E-enoate (**2a**):* yellowish oil (yield 56%). IR (KBr) $_{max}$ 3421, 2947, 2846, 1724, 1658, 1593, 1508, 1433, 1267, 1213, 1157, 1085, 1031 cm^{-1}; ^{1}H NMR ($CDCl_3$, 400 MHz): /ppm 7.10 (1H, dt, *J* = 15.5 and 6.8 Hz, H-8), 7.02 (1H, dt, *J* = 15.6 and 6.7 Hz, H-8'), 6.82 (1H, d, *J* = 8.1 Hz, H-6'), 6.76 (1H, d, *J* = 1.8 Hz, H-3'), 6.68 (1H, dd, *J* = 8.1 and 1.8 Hz, H-2'), 6.45 (1H, d, *J* = 1.8 Hz, H-2), 6.24 (1H, d, *J* = 1.8 Hz, H-6), 5.85 (1H, dt, *J* = 15.5 and 1.5 Hz, H-9), 5.77 (1H, dt, *J* = 15.6 and 1.5 Hz, H-9'), 3.87 (3H, s, H-10/10'), 3.82 (3H, s, H-13), 3.73 (3H, s, H-12), 3.71 (3H, s, H-12'), 3.50 (2H, dd, *J* = 6.7 and 1.0 Hz, H-7'), 3.37 (2H, dd, *J* = 6.8 and 1.2 Hz, H-7); ^{13}C NMR ($CDCl_3$, 100 MHz): /ppm 167.0 (C-11), 166.9 (C-11'), 153.9 (C-5'), 150.9 (C-4'), 150.8 (C-5), 147.6 (C-8), 147.4 (C-8'), 144.5 (C-3), 138.6 (C-4), 133.9 (C-1'), 133.2 (C-1), 122.1 (C-9'), 122.0 (C-9), 121.2 (C-2'), 119.8 (C-3'), 113.3 (C-6'), 111.7 (C-6), 107.8 (C-2), 61.1 (C-13), 56.3 (C-10), 56.1 (C-10'), 51.6 (C-12/12'), 38.4 (C-7), 38.5 (C-7'); ESI-HRMS *m/z* 479.1677 $[M + Na]^+$ (calcd. for $C_{25}H_{28}O_8Na$ 479.1682); Anal. C 65.55, H 6.20% (calcd. for $C_{25}H_{28}O_8$, C 65.78, H 6.18%).

2.5. Experimental animals

BALB/c mice were obtained by the animal breeding facility at the Instituto Adolfo Lutz - São Paulo State, Brazil. The animals were maintained in sterilized boxes with absorbent material under a controlled environment and received water and food *ad libitum*. BALB/c mice were used to obtain peritoneal macrophages, and for *T. cruzi* maintenance infection [16]. Animal procedures were performed with the approval of the

Research Ethics Commission (project CEUA-IAL 05/2018), in agreement with the Guide for the Care and Use of Laboratory Animals from the National Academy of Sciences.

2.6. Parasites and mammalian cell maintenance

T. cruzi trypomastigotes (Y strain) were maintained in Rhesus monkey kidney cells (LLC-MK2 – ATCC CCL 7), using RPMI-1640 medium supplemented with 2% fetal bovine serum (FBS) at 37 ºC in a 5% CO_2-humidified incubator. Murine conjunctive cells (NCTC clone 929, ATCC) and LLC-MK2 were maintained in RPMI-1640 supplemented with 10% FBS at 37 ºC in a 5% CO_2-humidified incubator. Macrophages were obtained from the peritoneal cavity of BALB/c mice by washing them with RPMI-1640 medium supplemented with 10% FBS and were maintained at 37 ºC in a 5% CO_2-humidified incubator [17].

2.7. Determination of anti-trypomastigote and anti-amastigote activity

The 50% effective concentration (EC_{50}) of compounds **1**, **1a, 2**, and **2a** against *T. cruzi* was determined in trypomastigotes and amastigotes forms. Trypomastigotes were obtained from LLC-MK2 cultures previously infected. The parasites were counted in a Neubauer hemocytometer, seeded at 1 x 10^6 cells/well (96-well plates), and incubated with serial dilutions of the tested compounds (150 – 1.71 µM), for 24 h at 37 ºC in a 5% CO_2-humidified incubator, with benznidazole as the standard drug. The trypomastigote viability was evaluated by the resazurin (Sigma) assay [6]. To determine the activity against intracellular amastigotes, peritoneal macrophages from BALB/c mice were infected with trypomastigotes forms of *T. cruzi*. The macrophages obtained from the

peritoneal cavity of BALB/c mice were plated on a 16-well chamber slide (NUNC plate, Merck; 1 x 10^5/well) and incubated for 24 h at 37 ºC in a 5% CO_2-humidified incubator. Trypomastigotes obtained as described above, were washed in RPMI-1640 medium, counted, and used to infect the macrophages (parasite:macrophage, ratio = 10:1). After 2 h of incubation at 37 ºC in a 5% CO_2-humidified incubator, non-internalized parasites were removed by washing with the medium [17]. Compounds **1**, **1a**, **2**, and **2a** were individually incubated with infected macrophages (48 h at 37 ºC, 5% CO_2) at different concentrations using benznidazole as the standard drug. At the end of the assay, slides were fixed with MeOH and stained with Giemsa prior to counting under a light microscope (EVOS M5000, THERMO). EC_{50} values were calculated as described [6]. The data represent the mean of three independent assays, tested in duplicate. Infected macrophages without drug treatments were included as a negative control [17].

2.8. Determination of cytotoxicity against mammalian cells

The cytotoxicity determination of compounds **1**, **1a**, **2**, and **2a** was performed using NCTC cells-clone. The cells (6 x 10^4 cells/well, L929, passage 16) were seeded and incubated with tested compounds (200 – 1.56 µM) for 48 h at 37 ºC in a 5% CO_2 incubator. The 50% cytotoxic concentrations (CC_{50}) were determined by the 3-(4,5-dimethylthiazol-2-yl)-2,5-diphenyltetrazolium bromide (MTT) assay [6]. The optical density was determined in FilterMax F5 (Molecular Devices) at 570 nm. The selectivity index (SI) values were calculated for both forms of the parasite (trypomastigotes and amastigotes) using the equation: CC_{50} against L929 cells/EC_{50} against parasites. Cells without drug

treatments were included as a negative control. The data represent the mean of two independent assays, tested in duplicate [17].

2.9. Evaluation of plasma membrane electric potential (ΔΨp) in T. cruzi *trypomastigotes*

Evaluation of plasma membrane electric potential (ΔΨp) with bis-(1,3-diethylthiobarbituric acid)trimethine oxonol (DISBAC2 - 3) probe in *T. cruzi* trypomastigotes treated was performed for 2 h with compounds **1a** and **2a**. Controls of the assay were trypomastigotes treated with gramicidin (0.5 µg/mL) (positive control – C+) and untreated parasites (negative control – C-). Fluorescence was quantified by calculating the mean percentages of untreated (0%) and gramicidin-treated (100%) parasites. Evaluation of mitochondrial membrane potential in *T. cruzi* trypomastigotes was performed with **1a** and **2a** labeled with JC-1 probe (0.2 µM). Parasites without drug treatments were included as a negative control. The fluorescence was measured in a flow cytometer (ATTUNE) after 1 and 2 h of incubation with tested compounds. Controls of the assay were trypomastigotes treated with carbonylcyanide *m*-chlorophenylhydrasone (CCCP) at 100 µM (C+) and untreated parasites (C-). Fluorescence was quantified by calculating the ratio between the channels BL2/BL1. *$p < 0.05$. The data represent the mean of three independent assays, tested in duplicate [18].

2.10. Evaluation of Ca^{2+} *levels in* T. cruzi *trypomastigotes*

Fluo-4 acetoxymethyl ester (Flu4-AM) probe was measured spectrofluorimetrically (excitation 360 nm and emission 500 nm) by 260 min of incubation after treatment of

trypomastigotes with compounds **1a** and **2a** at IC_{50} value. Untreated trypomastigotes and treated with triton-X 100 (TX-100) at 0.5% were used as a negative (C-) and positive (C+) control, respectively. Fluorescence was reported as a percentage relative to untreated trypomastigotes (100%). Parasites without drug treatments were included as a negative control. The data represent the mean of three independent assays, tested in duplicate [18].

2.11. Statistical analysis

EC_{50} and CC_{50} data represent the mean of three independent representative assays tested in duplicate and were calculated using sigmoid dose-response curves in Graph–Pad Prism 6.0 software (San Diego, CA, USA). Mechanism of action studies were analyzed using ANOVA test turkey for significance ($p < 0.05$).

3. Results and discussion

Previous studies demonstrated the anti-*T. cruzi* activity of neolignans dehydrodieugenol B (**1**) and methyldehydrodieugenol B (**2**), both isolated from *Nectandra leucantha* [14]. Further studies also indicated that different semi-synthetic compounds, especially those containing chemical differences of the allyl side chain, displayed higher anti-*T. cruzi* potential in comparison with natural products **1** and **2** [19]. Inspired by our previous works on cross-metathesis of acrylic derivatives with unsaturated natural products [20 – 24] including 4-allylphenol substrates [25, 26], the cross-metathesis reaction was conducted with natural dehydrodieugenol B (**1**) and its methyl ether (**2**). This

procedure, catalyzed by the second generation Hoveyda catalyst [27] and dimethyl carbonate as solvent [28, 29] afforded new compounds **1a** and **2a** both containing an additional methoxycarbonyl group at C-9/C-9' (Figure 1) in 42 and 56% yield, respectively.

ESI-HRMS spectra of compounds **1a** and **2a,** showed $[M + Na]^+$ ion peaks at *m/z* 465.1519 and 479.1677, respectively, compatible with molecular formulas $C_{24}H_{26}O_8$ and $C_{25}H_{28}O_8$. ^1H NMR spectra of both derivatives exhibited similarities to those observed for compounds **1** and **2**, especially in the region of aromatic hydrogens in the range 6.88 – 6.24. However, the main detected difference was the presence of two coupled systems at 7.09 (ddt, *J* = 15.7 and 6.7 Hz) and 5.84 (d, *J* = 15.7 Hz), assigned to H-8/8´ and H-9/9´, respectively. Based on the value of the coupling constant between H-8/8' and H-9/9' (15.7 Hz), it was possible to infer the *E* stereochemistry of both double bonds [30]. Furthermore, the presence of one singlet at 3.71 (6H) was indicative of two additional methoxy groups, attributed to H-12/12´. Analysis of ^{13}C NMR spectra indicated also the similarities between these compounds and natural products **1** and **2**, especially signals attributed to the carbons of aromatic rings ranging from 154 to 107. However, the presence of methoxycarbonyl unity was confirmed by the presence of additional signals at 167.0 (C-11/11´) and 51.6 (C-12/12´). Therefore, structures of compounds **1a** and **2a** were determined, respectively, as methyl 4-{4-[2-hydroxy-3-methoxy-5-(4-methoxy-4-oxobut-2*E*-en-1-yl)phenoxy]-3-methoxyphenyl}but-2*E*-enoate and methyl 4-{4-[2,3-dimethoxy-5-(4-methoxy-4-oxobut-2*E*-en-1-yl)phenoxy]-3-methoxyphenyl}but-2*E*-enoate, as shown in Figure 1.

Compounds **1a** and **2a** were effective in killing trypomastigotes of *T. cruzi* with EC_{50} values of 13.5 and 23.0 M, respectively, as observed in Table 1. Furthermore, compound **1a** showed moderate cytotoxicity (CC_{50} of 139.8 M) while compound **2a** was non-toxic

to the highest tested concentration of 200 μM. Considering the selectivity index (SI), which is the relation between the cytotoxicity in NCTC cells and the activity against trypomastigote forms, it was possible to calculate values of 10.3 and > 8.7 for compounds **1a** and **2a**, respectively. When tested against the intracellular amastigotes, the most relevant clinical form of *T. cruzi*, compounds **1a** and **2a** exhibited high potential, with EC_{50} values of 10.2 and 6.1 μM, respectively, superior to the positive control benznidazole (IC_{50} of 18.7 μM) ($p<0.05$). Concerning the toxicity against NCTC cells, compounds **1a** and **2a** displayed SI values of 13.7 and > 32.8, respectively, higher than those calculated for benznidazole (SI > 10.7) ($p<0.05$). Considering chemical structures of natural products **1** and **2** and derivatives **1a** and **2a**, the inclusion of the methoxycarbonyl group at the allyl side chain of natural neolignans provided considerable impact on parasite activity, especially against amastigote forms of *T. cruzi*. As presented in Table 1, an increment in the potency of the derivative **1a** (EC_{50} of 10.2 μM) in comparison to natural product **1** (EC_{50} of 86.5 μM) was observed ($p<0.05$), but with higher toxicity against NCTC cells (CC_{50} of 139.8 μM) ($p<0.05$), a similar effect already observed with other chemically related phenolic derivatives [7]. The increment in the bioactivity caused by chemical derivatization was more intense when EC_{50} values of compounds **2** and **2a** were compared ($p<0.05$). As observed, natural product **2** showed to be inactive against both trypomastigote and amastigote forms of *T. cruzi* (EC_{50} > 150 μM) while compound **2a** exhibited excellent potential (EC_{50} of 6.1 μM) and reduced toxicity (CC_{50} > 200 μM). Considering these results, it could be suggested that methoxycarbonyl unity plays an important role in the anti-*T. cruzi* activity, especially against amastigote forms of this parasite. Based on the obtained results and the criteria preconized by the Drug for Neglected Diseases initiative (DNDi) [31] for the discovery of new hit compounds for *T. cruzi* that include EC_{50} values

lower than 10 μM against amastigotes and SI >10, it is possible to suggest that derivative **2a** could be considered a hit compound for future chemical optimizations for Chagas disease.

Considering the potency of compounds **1a** and **2a**, different assays were performed to evaluate their mechanism of action on the trypomastigotes. The plasma membrane is the first contact of an exogenous compound with the cell and damage to its structure can lead to irreversible effects. Using the SYTOX Green fluorescent probe, compounds **1a** and **2a** showed no interference in the permeability of the plasma membrane permeability (data not shown), differently from that observed for 1-[(7S)-hydroxy-8-propenyl]-3-[3'-methoxy-1'-(8'-propenyl)-phenoxy]-4,5-dimethoxybenzene, a natural neolignan isolated from *N. leucantha*, but structurally different of compound **2** due to the presence of an additional hydroxyl group at C-7 position [14]. However, compounds **1a** and **2a** caused a significant depolarization of the plasma membrane electric potential, similar to that observed in chemically related neolignans isolated from *N. leucantha* [14] as well as their semi-synthetic derivatives [19]. As observed in figure 2, compound **1a** induced the disturbance after 2 h of incubation ($p < 0.001$), whereas with compound **2a** it was only after 1 h of incubation ($p < 0.05$). This effect might be ascribed to a transient depolarization caused by **2a** in the membrane, which reverted to a homeostasis after this period. The membrane potential is the result of the movement of numerous ions through ion channels and transporters, resulting in different electrostatic charges across the cell membrane. The maintenance of plasma membrane integrity is essential for normal cell viability and function and damage can directly affect the homeostasis [32].

Differently from the mammalian cells, Trypanosomatidae parasites present a unique mitochondrion, being considered an interesting target for drug discovery studies

[33]. Using JC1 as a fluorescent probe, compounds **1a** and **2a** showed a depolarization of the mitochondrial membrane potential (ΔΨm) after 1 h of incubation (Figure 3A). Undoubtedly, cell life critically depends on the maintenance of the mitochondrial membrane potential. If the repair machinery starts a robust response, this electric potential can be restored. Compounds **1a** and **2a** were incubated for more than 1 h, but the depolarization effect continued even after 2 h treatment (Figure 3B). The ΔΨm is generated by proton pumps and is an essential component in the process of energy storage during oxidative phosphorylation. However, continued changes may be deleterious, resulting in the loss of cell viability [34].

Intracellular calcium participates in the different processes including cell differentiation, proliferation, and motility. It can be altered in response to a number of stimuli including chemical, electrical, and physical. Alterations of these levels can trigger specific cellular responses, affecting cell viability [35]. In this study, the *T. cruzi* Ca^{2+} levels after treatment with compounds **1a** and **2a** were also investigated, but no alterations could be observed after 2 h (data not shown), suggesting other initial targets rather than calcium storage organelles like acidocalcisomes.

4. Conclusion

In this work, dehydrodieugenol B (**1**) and its methyl ether (**2**), both isolated from *N. leucantha*, were used as starting material for the preparation of derivatives **1a** and **2a** via olefin cross-metathesis reaction. These modified compounds showed a promising trypanocidal effect, with antiparasitic selectivity and affecting the unique mitochondrial system of the parasite. Especially for compound **2a**, insertion of the methoxycarbonyl

group resulted in a promising efficiency without mammalian cytotoxicity. Mechanism of action studies of both compounds **1a** and **2a** demonstrated a depolarization of the plasma membrane potential, followed by a mitochondrial membrane potential collapse. On the other hand, neither Ca^{2+} level nor ROS alterations were observed after a short-time incubation. Considering the hit criteria for new candidates, tested compounds but especially derivative **2a,** could be considered prototypes for optimization studies for the design of new derivatives against *T. cruzi*.

Acknowledgments

The authors acknowledge CAPES−COFECUB for support to the project no. PHC 884-17 (France) and 883/2017 (Brazil), CNPq (project 312288/2019-0 and 404843/2018-2); FAPESP (2021/02789-7, 2021/04464-8, 2018/01258-5, 2018/07885-1, 2018/10279-6, 2017/24931-4, 2017/17044-1, and 2016/05006-5), CAPES (Finance Code 001), Institutional Internationalization Program CAPES-PrInt/UFABC and the Multi-User Central Facilities (CEM/UFABC) for the experimental support. J.H.G.L., A.G.T. and D.M. also thank CNPq for fellowships. Finally, T. S. G. thanks the CAPES−COFECUB grant 88887.198050/2018-00. Umicore is thanked for supplying the ruthenium catalyst. This study is an activity within the Research Network Natural Products against Neglected Diseases (ResNetNPND: http://www.resnetnpnd.org/).

Declaration of Competing Interest

The authors declare that they have no known competing financial interests or personal relationships that could have appeared to influence the work reported in this paper.

References

[1] R. W. Peeling, D. I. Boeras, J. Nkengasong, Re-imagining the future of diagnosis of Neglected Tropical Diseases. Comput. Struct. Biotechnol. J. 15 (2017) 271-274.

[2] E. Chatelain, J-R. Ioset, Drug discovery and development for neglected diseases: the DNDi model. Drug Dis. Dev. Ther. 5 (2011) 175-181.

[3] F. R. Martins-Melo, A. N. Ramos Jr., C. H. Alencar, J. Heukelbach, Mortality from neglected tropical diseases in Brazil, 2000-2011. Bull. World Health Org. 94 (2016) 103-110.

[4] P. A. Sales Junior, I. Molina, S. M. F. Murta, A. Sánchez-Montalvá, F. Salvador, R. Corrêa-Oliveira, C. M. Carneiro, Experimental and clinical treatment of Chagas disease: A review. Am. J. Trop. Med. Hyg. 97 (2017) 1289-1303.

[5] G. A. A. Conserva, T. A. Costa-Silva, M. Amaral, G. M. Antar, B. J. Neves, C. H. Andrade, A. G. Tempone, J. H. G. Lago, Butenolides from *Nectandra oppositifolia* (Lauraceae) displayed anti-*Trypanosoma cruzi* activity via deregulation of mitochondria. Phytomedicine 54 (2019) 54, 302-307.

[6] V. S. Londero, T. A. Costa-Silva, K. S. Gomes, D. D. Ferreira, J. T. Mesquita, A. G. Tempone, M. C. M. Young, G. Jerz, J. H. G. Lago, Acetylenic fatty acids from *Porcelia*

macrocarpa (Annonaceae) against trypomastigotes of *Trypanosoma cruzi*: Effect of octadec-9-ynoic acid in plasma membrane electric potential. Bioorg. Chem. 78 (2018) 307-311.

[7] S. S. Grecco, T. A. Costa-Silva, G. Jerz, F. S. Sousa, G. A. A. Conserva, J. T. Mesquita, M. K. Galuppo, A. G. Tempone, B. J. Neves, C. H. Andrade, R. L. O. R. Cunha, M. Uemi, P. Sartorelli, J. H. G. Lago, Antitrypanosomal activity and evaluation of the mechanism of action of dehydrodieugenol isolated from *Nectandra leucantha* (Lauraceae) and its methylated derivative against *Trypanosoma cruzi*. Phytomedicine 24 (2017) 62-67.

[8] S. S. Grecco, H. Lorenzi, A. G. Tempone, J. H. G. Lago, Update: biological and chemical aspects of *Nectandra* genus (Lauraceae). Tetrahedron: Asymmetry 27 (2016) 793-810.

[9] J. B. Baitello, F. G. H. Hernández, P. L. R. Moraes, R. Esteves, J. R. Marcovino, In Flora Fanerogâmica do Estado de São Paulo; Wanderley, M. G. L.; Shepherd, G. J.; Melhem, T. S.; Giulietti, A. M.; Kirizawa, M., eds.; RiMA/FAPESP 3 (2003) 149-223.

[10] A. Quinet, J. B. Baitello, P. L. R. Moraes, L. Assis, F. M. Alves, Lauraceae in Lista de Espécies da Flora do Brasil. 2015. Available at: http://floradobrasil.jbrj.gov.br/jabot/floradobrasil/FB8425

[11] M. I. Bittencourt-Mernak, N. M. Pinheiro, R. C. da Silva, V. Ponci, R. Banzato, A. J. M. C. R. Pinheiro, C. R. Olivo, I. F. L. C. Tibério, L. G. Lima Neto, F. P. R. Santana, J. H. G. Lago, C. M. Prado, Effects of eugenol and dehydrodieugenol B from *Nectandra leucantha* against lipopolysaccharide (LPS)-induced experimental acute lung inflammation. J. Nat. Prod. 84 (2021) 2282-2294.

[12] F. S. Sousa, S. S. Grecco, N. Girola, R. A. Azevedo, C. R. Figueiredo, J. H. G. Lago, Neolignans isolated from *Nectandra leucantha* induce apoptosis in melanoma cells by disturbance in mitochondrial integrity and redox homeostasis. Phytochemistry 140 (2017) 108-117.

[13] T. A. Costa-Silva, S. S. Grecco, F. S. Sousa, J. H. G. Lago, E. G. Martins, C. A. Terrazas, S. Varikuti, K. L. Owens, S. M. Beverley, A. R. Satoskar, A. G. Tempone, Immunomodulatory and antileishmanial activity of phenylpropanoid dimers isolated from *Nectandra leucantha*. J. Nat. Prod. 78 (2015) 653-657.

[14] S. S. Grecco, T. A. Costa-Silva, G. Jerz, G.; F. S. Sousa, V. S. Londero, M. K. Galuppo, M. L. Lima, J. B. Neves, C. H. Andrade, A. G. Tempone, J. H. G. Lago, Neolignans from leaves of *Nectandra leucantha* (Lauraceae) display in vitro antitrypanosomal activity via plasma membrane and mitochondrial damages. Chem. Biol. Int. 277 (2017) 55-61.

[15] L. S. Fernandes, D. Mandelli, W. A. Carvalho, C. Fischmeister, C. Bruneau. Functionalization of (-)-β-pinene and (-)-limonene via cross metathesis with symmetrical internal olefins. Catal. Commun., 135 (2020) 105893.

[16] S. S. Grecco, J. Q. Reimão, A. G. Tempone, P. Sartorelli, P. Romoff, M. J. P. Ferreira, O. A. Fávero, J. H. G. Lago, Isolation of an antileishmanial and antitrypanosomal flavanone from the leaves of *Baccharis retusa* DC. (Asteraceae). Parasitology Research, 106 (2010) 111-113.

[17] A. Rea, A. G. Tempone, E. G. Pinto, J. T. Mesquita, L .G. Silva, E. Rodrigues, P. Sartorelli, J. H. G. Lago. Soulamarin isolated from *Calophyllum brasiliense* (Clusiaceae) induces plasma membrane permeabilization of *Trypanosoma cruzi* and mytochondrial dysfunction. PLoS Negl. Trop. Dis. 7 (2013) e2556-e2563.

[18] T. A. Costa-Silva, M. L. Silva, G.M. Antar, A. G. Tempone, J. H. G. *Ent*-kaurane diterpenes isolated from *n*-hexane extract of *Baccharis sphenophylla* by bioactivity guided fractionation target the acidocalcisomes in *Trypanosoma cruzi*. Phytomedicine 93 (2021) 153748.

[19] D. D. Ferreira, F. S. Sousa, T. A. Costa-Silva, J. Q. Reimão, A. C. Torrecilhas, D. M. Johns, C. E. Sear, K. M. Honorio, J. H. G. Lago, E. A. Anderson, A. G. Tempone, Dehydrodieugenol B derivatives as antiparasitic agents: Synthesis and biological activity against *Trypanosoma cruzi*. Eur. J. Med. Chem. 176 (2019) 162–174.

[20] C. Bruneau, C. Fischmeister, Alkene metathesis for transformations of renewables. Top. Organomet. Chem. 63 (2019) 77-102.

[21] X. Miao, R. Malacea, C. Fischmeister, C. Bruneau, P. H. Dixneuf, Ruthenium–alkylidene catalysed cross metathesis of fatty acid derivatives with acrylonitrile and methyl acrylate: a key step toward long-chain bifunctional and amino acid compounds. Green Chem. 13 (2011) 2911-2919.

[22] X. Miao, C. Fischmeister, P H. Dixneuf, C. Bruneau, J. L. Dubois, J. L. Couturier, Polyamide precursors from renewable 10-undecenenitrile and methyl acrylate via olefin cross metathesis. Green Chem. 14 (2012) 2179-2183.

[23] C. Bruneau, C. Fischmeister, D. Mandelli, W. A. Carvalho, E. N. dos Santos, P.H. Dixneuf, L. Sarmento-Fernandes, Transformations of terpenes and terpenoids via carbon–carbon double bond metathesis. Cat. Sci. Technol. 8 (2018), 3989-4004.

[24] L. S. Fernandes, D. Mandelli, W. A. Carvalho, E. Caytan, C. Fischmeister, C. Bruneau, Cross metathesis of (-)-β-pinene, (-)-limonene and terpenoids derived from limonene with internal olefins. Appl. Cat. A Gen. 623 (2021) 118284.

[25] H. Bilel, N. Hamdi, C. Fischmeister, C. Bruneau, Transformations of bio-sourced 4 hydroxyphenylpropanoids based on olefin metathesis. ChemCatChem 12 (2020) 5000-5021.

[26] H. Bilel, N. Hamdi, F. Zagrouba, C. Fischmeister, C. Bruneau, Eugenol as a renewable feedstock for the production of polyfunctional alkenes via olefin cross metathesis. RSC Adv. 2 (2012) 9584-9589.

[27] S. B. Garber, J. S. Kingsbury, B. L. Gray, A. H. Hoveyda, Efficient and Recyclable Monomeric and Dendritic Ru-Based Metathesis Catalysts. J. Am. Chem. Soc. 122 (2000) 8168-8179.

[28] H. Bilel, N. Hamdi, F. Zagrouba, C. Fischmeister, C. Bruneau, Cross metathesis transformations of terpenoids in dialkyl carbonate solvents. Green Chem. 13 (2011) 1448-1452.

[29] X. Miao, C. Fischmeister, C. Bruneau, P. H. Dixneuf, Dimethyl carbonate: an eco-friendly solvent in ruthenium-catalyzed olefin metathesis transformations. ChemSusChem 1 (2008) 813-816.

[30] G. J. Martin, M. L. Martin, The stereochemistry of double bonds, Prog. Nucl. Magn. Reson. Spectrosc. 8 (1972) 166-259.

[31] R. Don, J. R. Ioset, Pathogenesis of Chagas' disease: parasite persistence and autoimmunity. Parasitology 141 (2014) 140-146.

[32] S. H. Wright, Generation of resting membrane potential. Adv. Physiol. Educ. 28 (2004) 139-142.

[33] L. M. Fidalgo, L. Gille, Mitochondria and trypanosomatids: Targets and drugs. Pharm. Res. 28 (2011) 2758-2770.

[34] L. D. Zorova, V. A. Popkov, E. Y. Plotnikov, D. N. Silachev, I. B. Pevzner, S. S. Jankauskas, V. A. Babenko, S. D. Zorov, A. V. Balakireva, M. Juhaszova, S. J. Sollott, D. B. Zorov, Mitochondrial membrane potential. Anal. Biochem. 552 (2018) 50-59.

[35] R. Bagur, G. Hajnóczky, Intracellular Ca^{2+} sensing: Its role in calcium homeostasis and signaling. Mol. Cell. 66 (2017) 780-788.

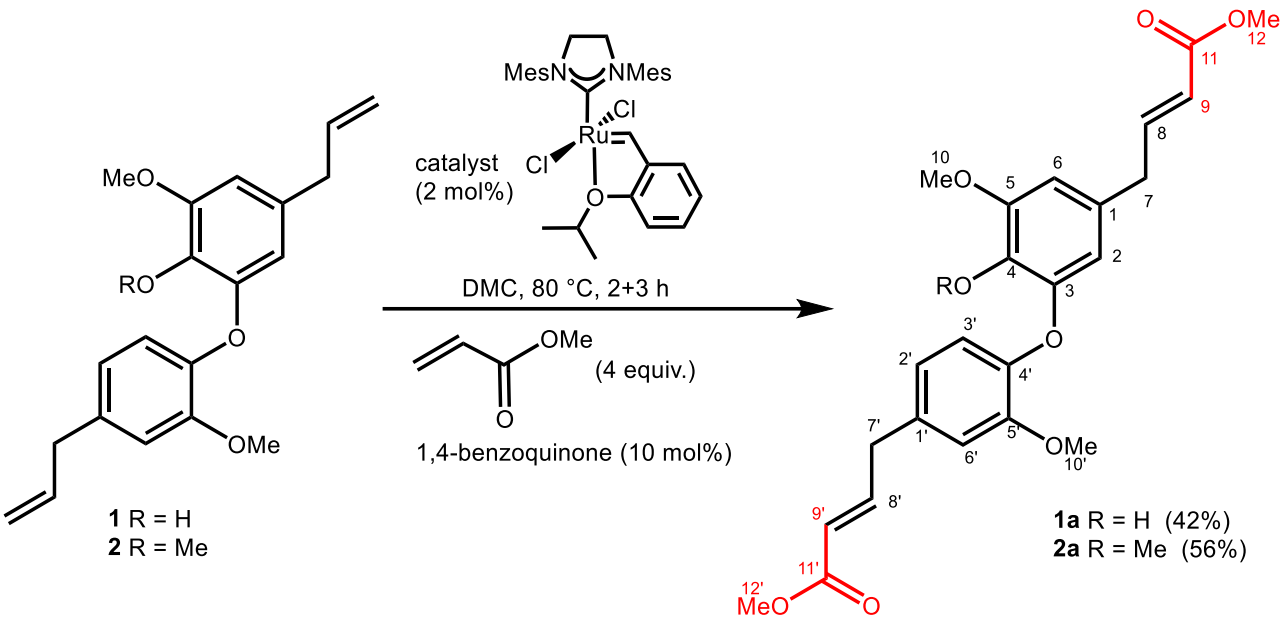

Figure 1. Chemical structures of derivatives **1a** and **2a** (in red - addition of methoxycarbonyl group) prepared by olefin cross-metathesis reaction from natural products **1** and **2**, isolated from twigs of *N. leucantha*

(chemical structures were drawn using ChemDraw Ultra 12.0)

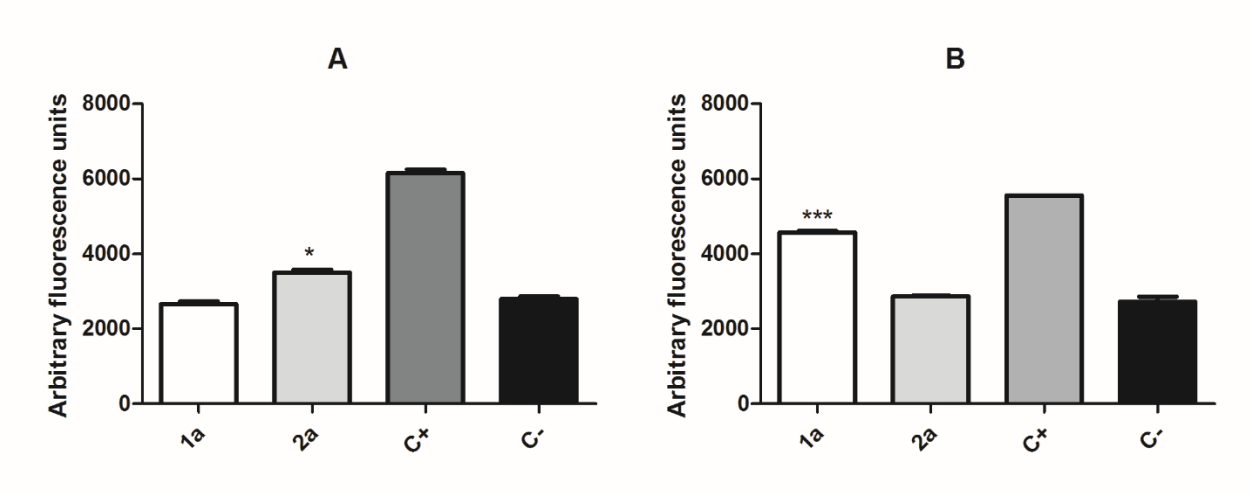

Figure 2. Evaluation of plasma membrane electric potential (ΔΨp) with DISBAC2 (3) probe in *T. cruzi* trypomastigotes treated for 1 h (A) and 2 h (B) of incubation with compounds **1a** and **2a.** Parasites were treated with gramicidin as a positive control, and with a drug-free medium as a negative control. A representative experiment is shown. * $p < 0.05$; *** $p < 0.001$

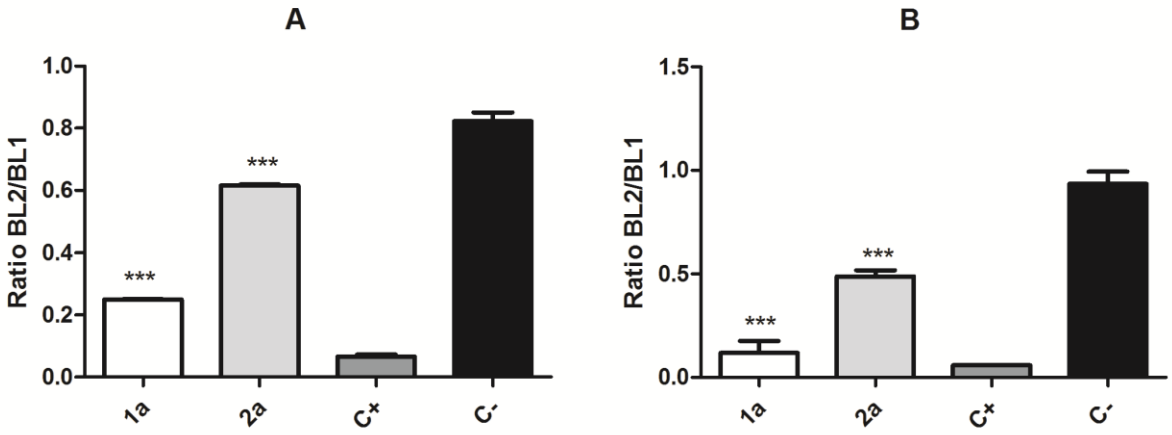

Figure 3. Evaluation of mitochondrial membrane potential (ΔΨm) in *T. cruzi* trypomastigotes treated with compounds **1a** and **2a** labeled with JC-1 probe (0.2 μM) for (A) 1h and 2 h (B) incubation. A representative experiment is shown. *** $p < 0.001$.

Table 1. Anti-*T. cruzi* activity (trypomastigotes and amastigotes) and cytotoxicity (NCTC cells) for positive control benznidazole (BZD), for natural products **1** and **2** as well as for derivatives **1a** and **2a.**

	EC_{50} (μM)		**CC_{50} (μM)**	**SI**	
	trypomastigote	amastigote	NCTC	trypomastigote	amastigote
1	38.6 ± 13.6	86.5 ± 10.4	> 200	> 5.2	> 2.3
1a	13.5 ± 11.0	10.2 ± 2.8	139.8 ± 19.3	10.3	13.7
2	NA	NA	> 200	-	-
2a	23.0 ± 2.1	6.1 ± 0.7	> 200	> 8.7	> 32.8
BZD	5.5 ± 0.9	18.7 ± 4.1	> 200	> 36.4	> 10.7

EC_{50} – 50% effective concentration, CC_{50} – 50% cytotoxic concentration, SI – selectivity index, calculated by the ratio CC_{50} against NCTC cells/EC_{50} against parasites (trypomastigote and amastigote forms), NA – not active at the higher tested concentration (150 μM).

SUPPLEMENTARY INFORMATION

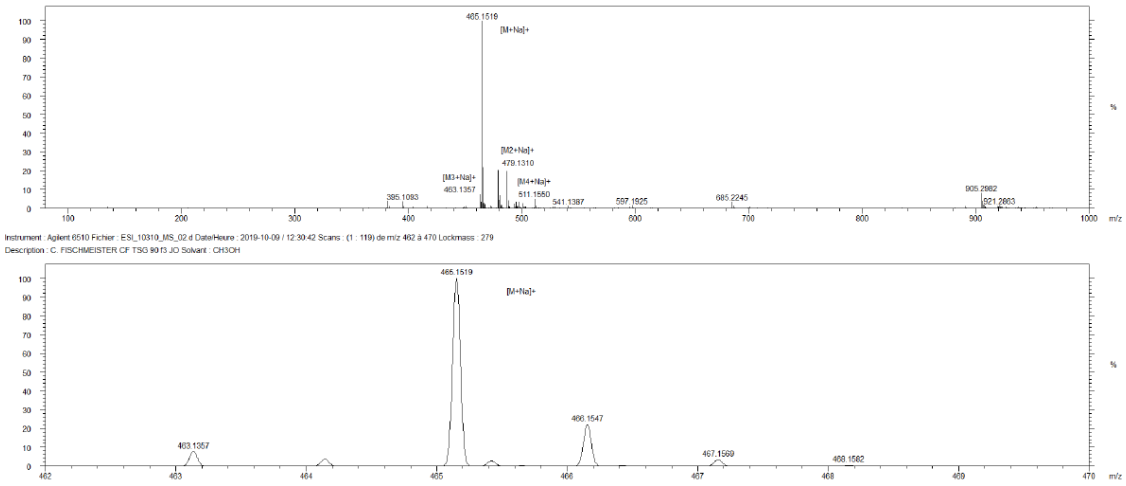

Figure S1. Positive mode ESI-qTOF-MS of compound **1a**.

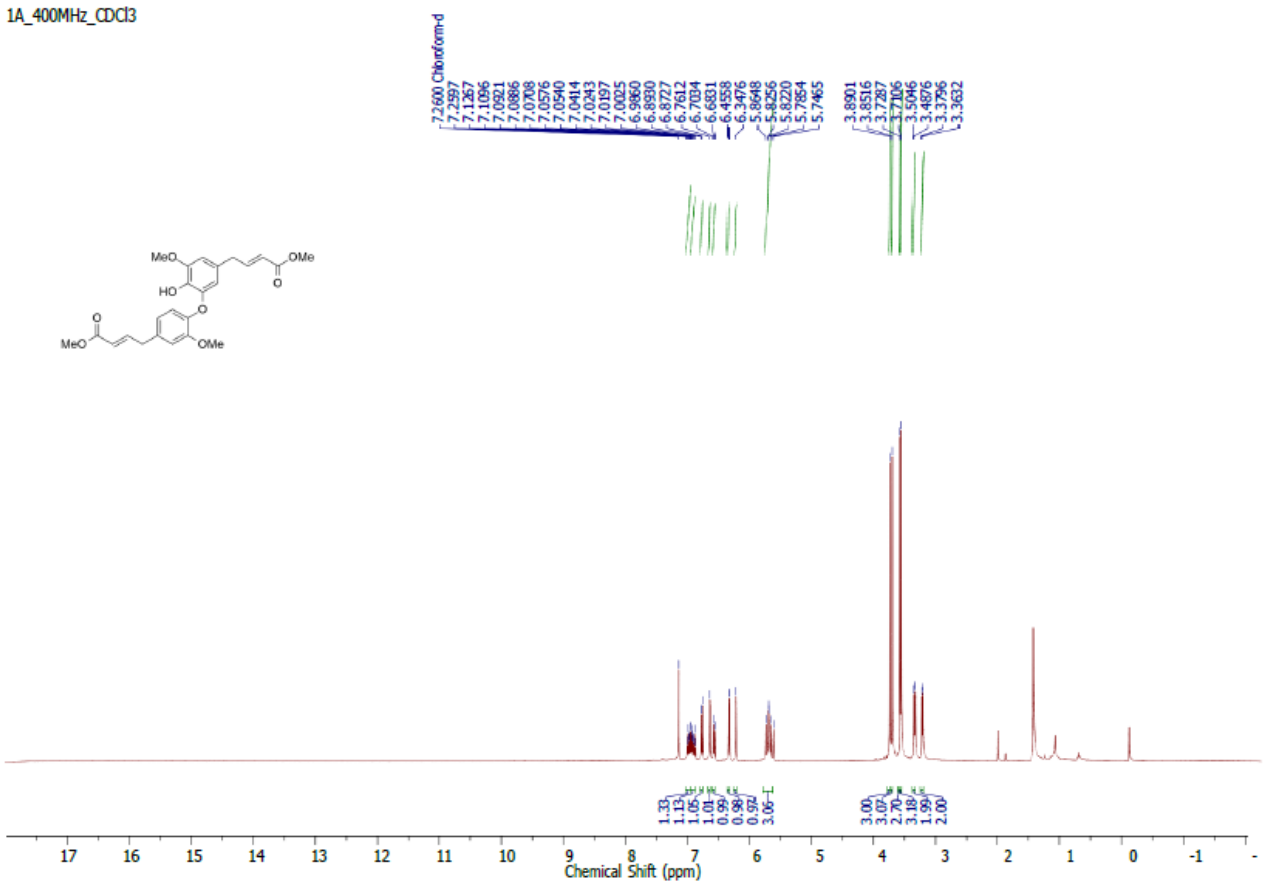

Figure S2. ^{1}H NMR spectrum (400 MHz, $CDCl_3$) of compound **1a**.

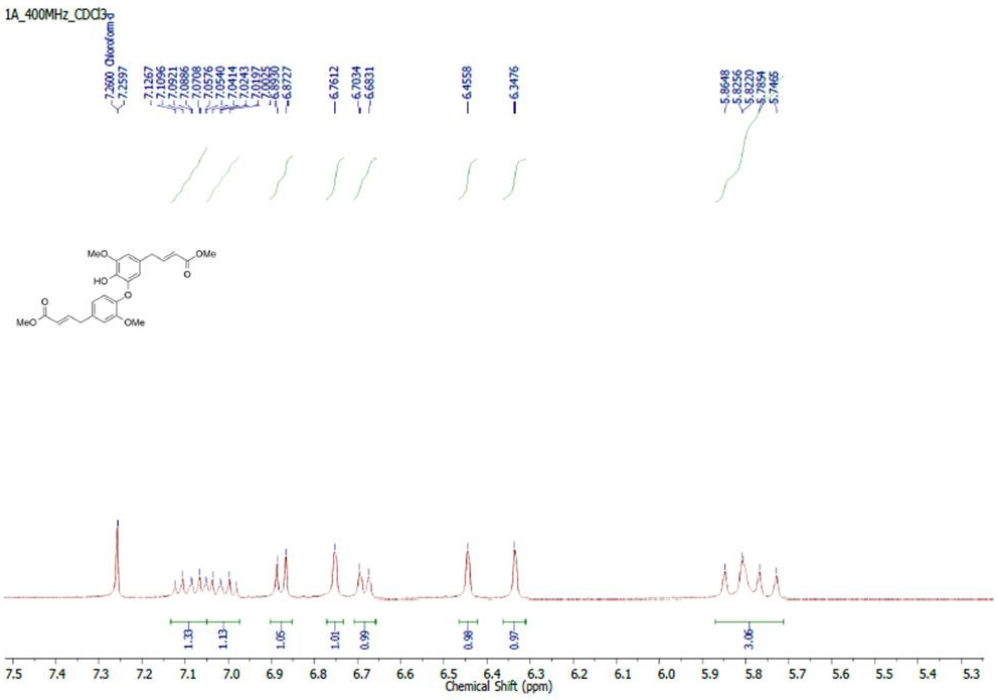

Figure S3. ^{1}H NMR spectrum (400 MHz, $CDCl_3$) of compound **1a**

(expansion of region δ 7.5 – 5.3)

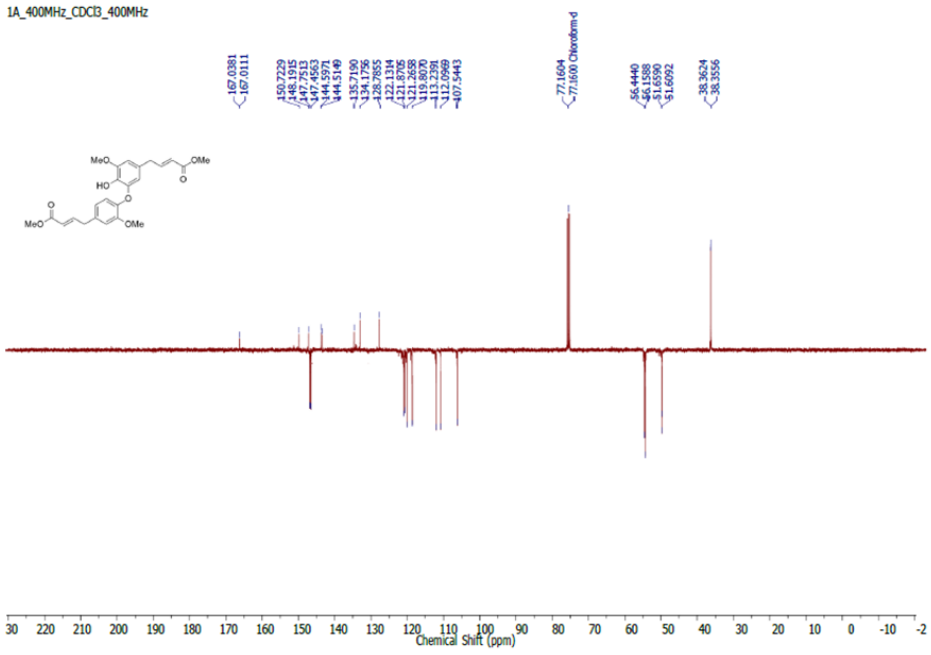

Figure S4. ^{13}C NMR spectrum (100 MHz, $CDCl_3$) of compound **1a**.

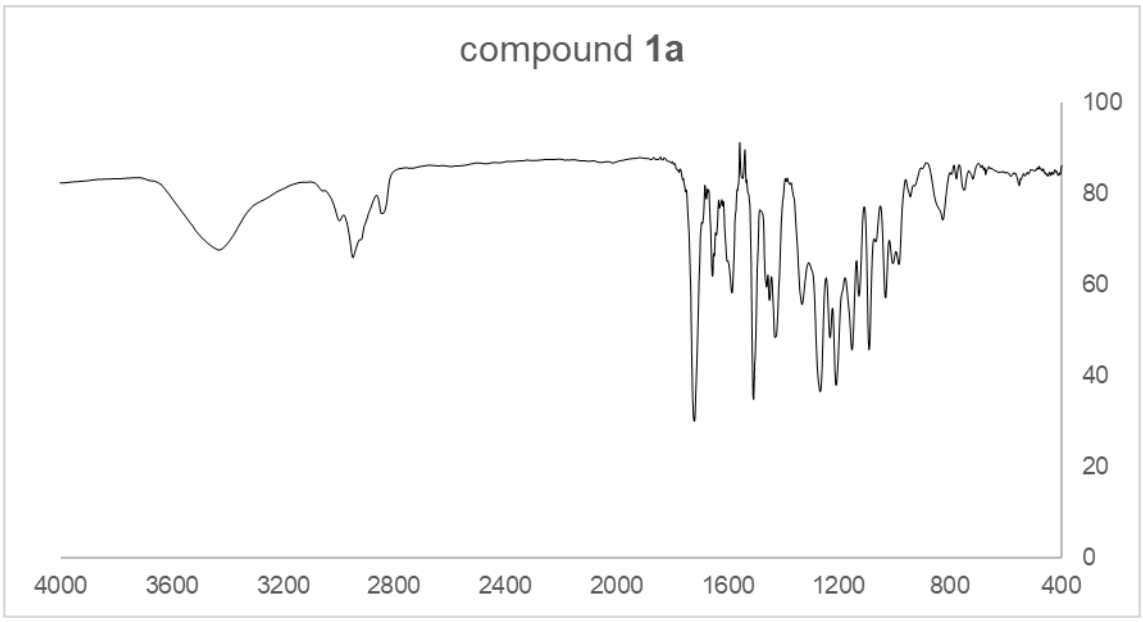

Figure S5. IR (KBr) spectrum of compound **1a**.

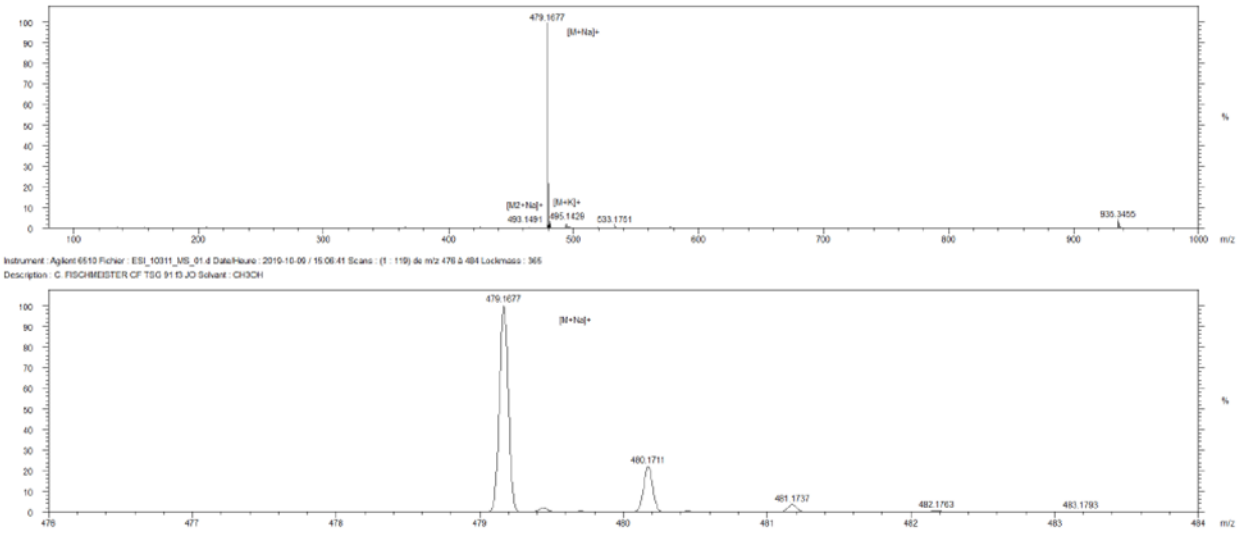

Figure S6. Positive mode ESI-qTOF-MS of compound **2a**.

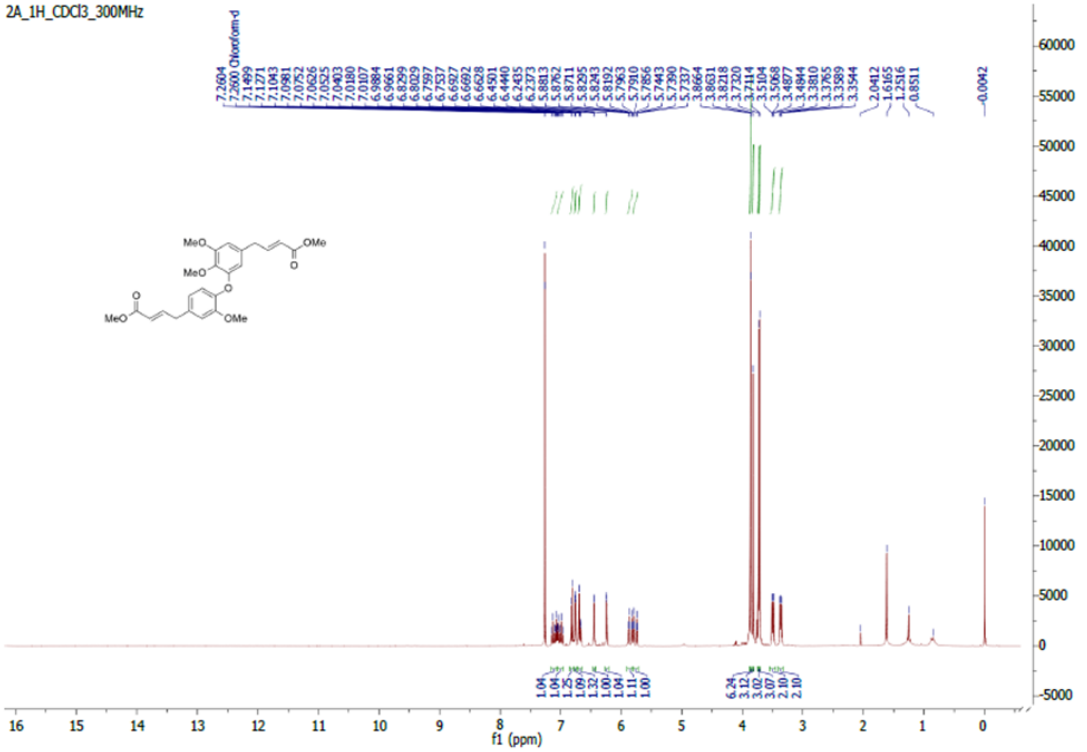

Figure S7. ^{1}H NMR spectrum (400 MHz, $CDCl_3$) of compound **2a**.

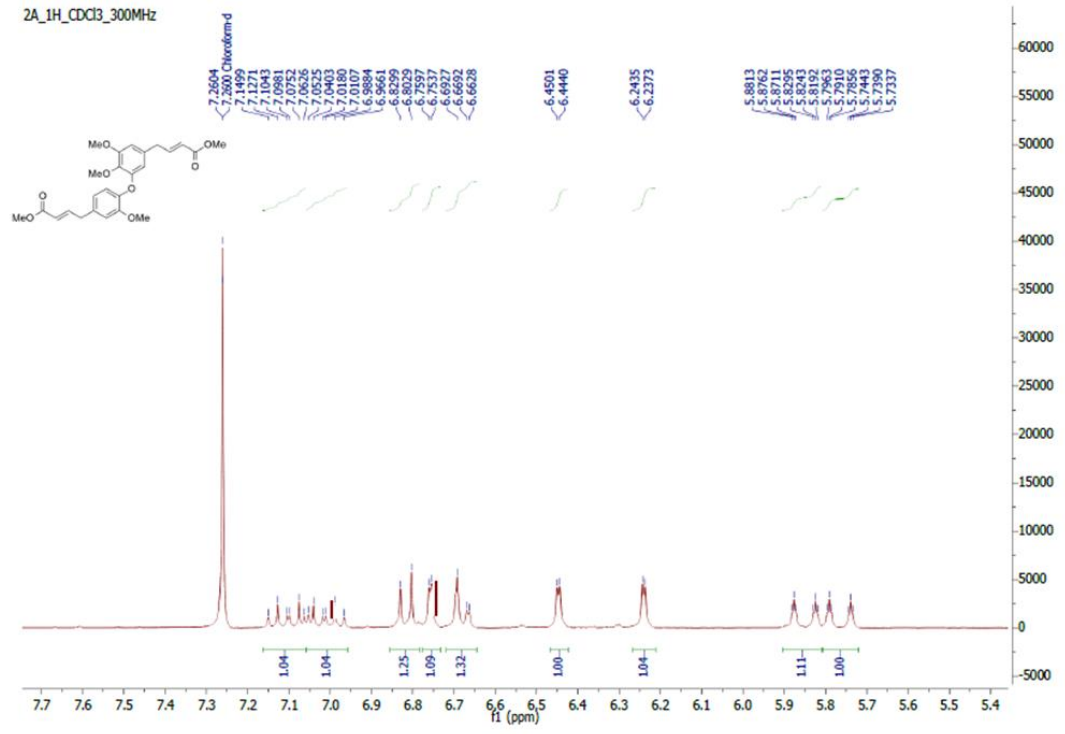

Figure S8. ^{1}H NMR spectrum (400 MHz, $CDCl_3$) of compound **2a**

(expansion of region δ 7.7 – 5.4)

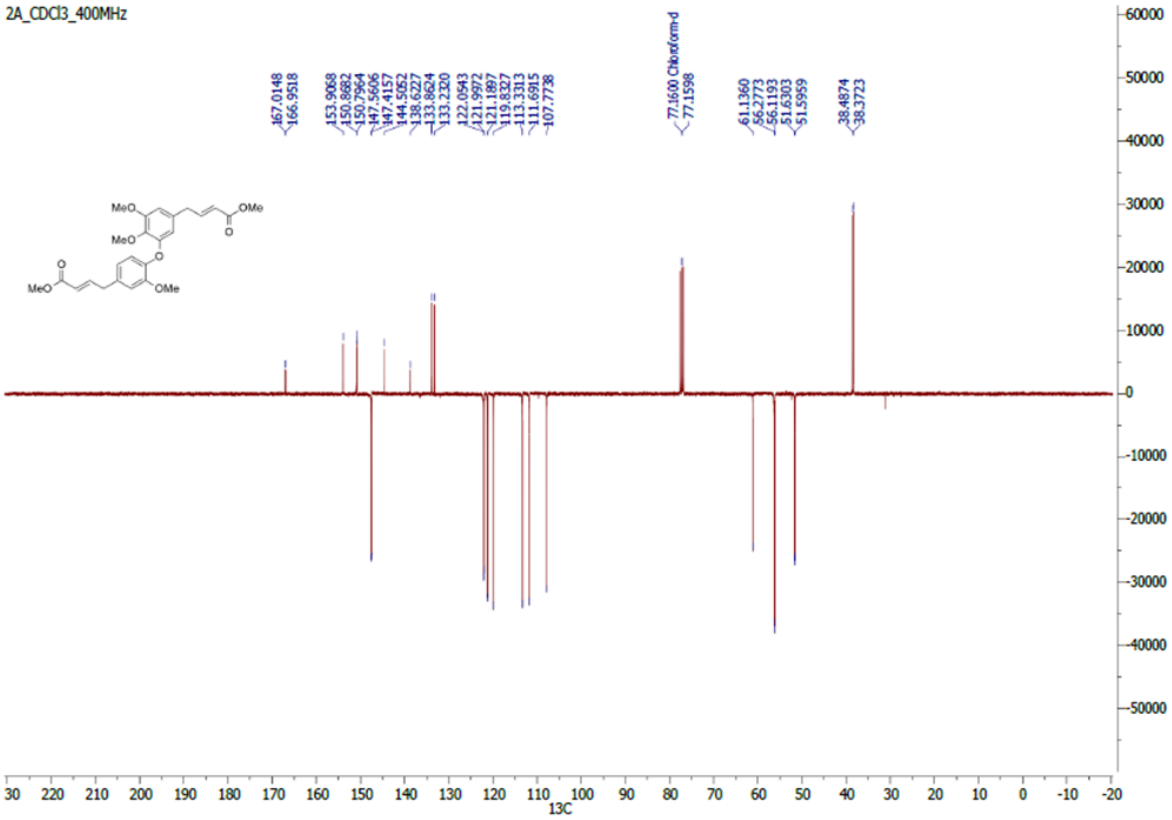

Figure S9. ^{13}C NMR spectrum (100 MHz, $CDCl_3$) of compound **2a**.

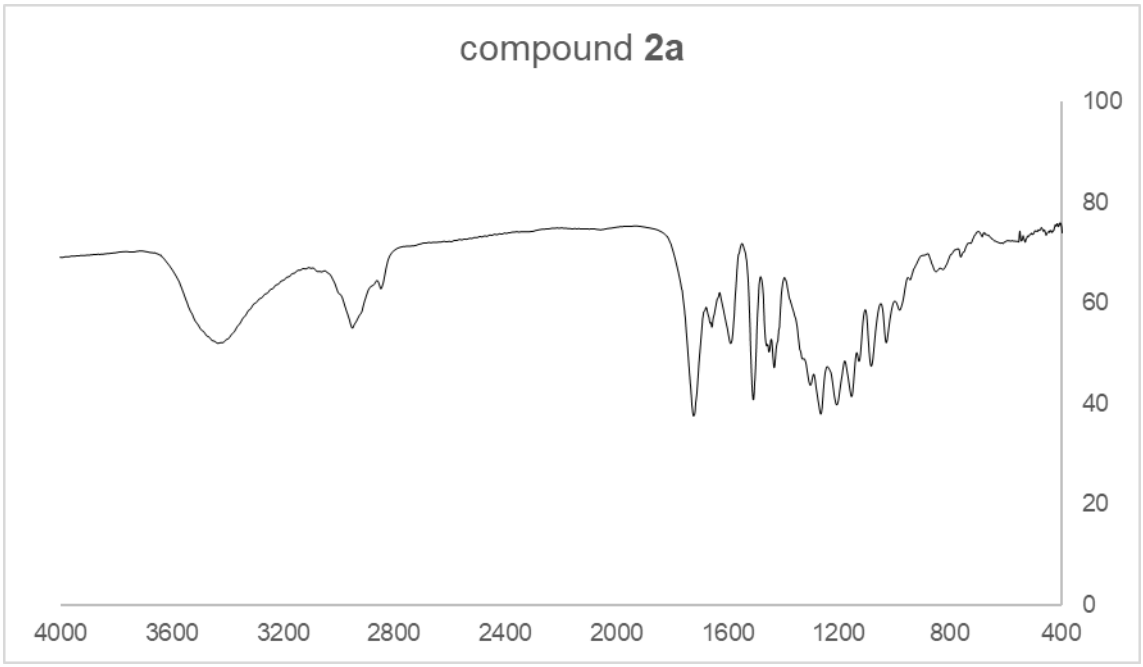

Figure S10. IR (KBr) spectrum of compound **2a**.